Proceedings of 5th Int'l Conf.
on Plasma Surface, May 3-5, 1982,
Gatlinburg, TN
Conf-820545--6

Trapping and Surface Permeation of Deuterium in Helium-Implanted Stainless Steel*

S. M. Myers and W. R. Wampler

Sandia National Laboratories
Albuquerque, NM 87185

SAND--82-0013C

DE82 014090

Abstract

Austenitic stainless steel was ion implanted with deuterium (D) and H and then heated, with the depth distribution of D being monitored via the nuclear reaction $^{2}D(^{3}He,p)^{4}He$. Analysis using diffusion theory indicated that D is bound to He-associated traps with an enthalpy of 0.42 $\pm$ 0.08 eV referenced to a solution site. The trapping entities are believed to be ~1 nm He bubbles observed by transmission electron microscopy, with D being bound to the bubble walls by a mechanism similar to chemisorption. Irradiation-defect traps, probably vacancies, exhibited a strength of only 0.22 $\pm$ 0.08 eV. Trapping behavior was essentially the same for types 304 and 310 stainless steel, indicating little dependence upon the stability of the austenitic (fcc) phase. The rate of D release at the surface was determined in the temperature range 425 - 575 K for two kinds of surface, one oxidized by electropolishing and air exposure, the other sputtered with Fe ions. Release was proportional to the square of solution concentration in both cases, but the recombination coefficient was $\gtrsim$100 times greater for the sputtered surface.

*This work performed at Sandia National Laboratories suported by the U. S. Department of Energy under contract number DE-AC04-76DP00789.

DISCLAIMER

INTRODUCTION

During operation of fusion reactors hydrogen isotopes will be ion-implanted from the plasma into stainless steel components. Temporary retention will be followed by release to the gas phase, and the rate of emission will affect both tritium inventory and plasma fueling. The principal factors which control this recycling are diffusion, trapping, and surface recombination. The diffusivity is approximately the same for most austenitic (fcc) stainless steels and is relatively straightforward to measure[1], but the other two properties vary considerably with microstructure and surface treatment, and their determination has proved more difficult and controversial. Consequently there have been a number of investigations of trapping and surface permeation for hydrogen isotopes in austenitic stainless steels [See Ref. 2 and F. Waelbroeck in these proceedings for reviews.] Surface recombination coefficients obtained by various groups differ as much as four orders of magnitude, illustrating the experimental problems.

In the present investigation we ion-implanted He and deuterium (D) into types 304 and 310 stainless steel and then used the nuclear reaction $^{2}D(^{3}He,p)^{4}He$ to observe D migration during heating. One objective was to examine the influence of He upon trapping within the ion-irradiated region; we note that small He bubbles in both bcc Fe and fcc Ni have previously been found to bind D more strongly than irradiation defects[3,4]. A second goal was to determine the surface release rate as a function of temperature and of the concentration of D in solution. This paper outlines the results, with details to follow in a more extended publication.

Procedures in this work differed from those of earlier ion-beam studies. By observing the redistribution of D between two trapping layers during linear ramping of temperature, trapping effects were characterized independently of the influence of the surface permeation barrier. Surface release was then examined during isothermal annealing of thin foils, under conditions where the populations of trap and solution sites were almost in equilibrium, making the interpretation particularly straightforward. Trap strengths and surface recombination coefficients were extracted by applying the diffusion equation with appropriate trapping terms and boundary conditions. Transmission electron microscopy provided microstructural information.

TRAPPING

To examine the trapping of D in He-implanted 304 stainless steel, a solution-annealed and electropolished specimen of thickness 0.4 mm was implanted at room temperature with 6 x 10^{16} at./cm^2 of 750 keV ^{3}He and 4 x 10^{16} at./cm^2 of 15 keV ^{4}He, followed by implantation of 2 x 10^{16} at./cm^2 of 15 keV D at a temperature of ~120 K. Theoretically predicted depth profiles for the He and D[5,6] are shown in Fig. 1. Sample temperature was then ramped linearly upward at 2 K/min., and at 10 K intervals the depth distribution of the D was probed by bombarding with 700 keV ^{3}He and counting protons from the nuclear reaction ^{2}D(^{3}He,p)^{4}He. As seen from the depth-dependent nuclear cross section in Fig. 1, the proton yield measured the areal density of D within the near-surface implanted layers, but was not sensitive to D within the deeper He layer centered at 1.2 μm.

Data from the above experiment are plotted as open circles in Fig. 2, where two distinct stages are apparent. The first stage, at ~420 K, occured when D began to migrate away from implanted traps within the region probed by the nuclear reaction, 0 - ~0.4 μm. Prevented from escaping at the nearby surface by a permeation barrier, the D instead redistributed so as to occupy implanted traps at 1.2 μm as well as those ≲0.4 μm. Equilibration between these two regions is reflected by a plateau after the first stage. As the temperature rose further, D diffused into the underlying bulk of the 400 μm-thick sample, and also penetrated the surface barrier to some degree, producing the broad second stage.

The redistribution of D between implanted layers during the first stage was demonstrated by detailed depth profiling. In a separate experiment the temperature ramp was halted at 493 K, within the plateau between stages, and the specimen cooled to ~120 K. Proton yield was measured as a function of incident ^{3}He energy, whereupon deconvolution[7] yielded D concentration versus depth as shown in Fig. 3. (In this instance the implanted D fluence was only half that of Fig. 2, but the redistribution behavior was essentially the same for both doses.) The peaks in Fig. 3 are broadened due to the limited depth resolution of the profiling technique, but areas and average depths are believed correct. For comparison the theoretically predicted ranges of 15 keV ^{4}He and 750 keV ^{3}He are indicated by arrows.

The experiment yielding solid circles in Fig. 2 was like that of the open circles except that no 750 keV ^{3}He was implanted at 1.2 μm (See Fig. 1.). The absence of the deeper trapping layer suppressed the first of the two stages, the one attributed to redistribution between layers. This observation further supports our interpretation of the evolution.

The open triangles in Fig. 2 are from yet another linear-ramp experiment, this one identical to that yielding open circles except that there was no implantation of 15 keV ^{4}He (See Fig. 1.). In this case the 0 -0.4 μm layer probed by ion beam analysis contained D and irradiation damage but no He. As a result the temperature of the principal stage is seen to be reduced by ~100 K from that of the open circles, indicating that the defect traps bind D less strongly than do traps associated with He. This conclusion was reinforced by depth profiling of the D following completion of the ramp represented by the triangles. The profile showed that all of the D released from the region 0 - 0.4 μm had accumulated within the He-implanted layer at 1.2 μm.

The observation of exceptionally strong He-associated traps in stainless steel parallels earlier findings for Fe and Ni hosts[3,4]. As in those investigations, we propose that the traps are small He bubbles, and that the D is bound to the walls of these entities by a mechanism similar to chemisorption on a free surface. Transmission electron microscopy confirmed the presence of such bubbles in type 304 stainless steel, the size being ~1 nm.

The theoretical curves in Fig. 2 were obtained from a set of coupled differential equations which describe diffusion within a field of traps. This formalism[7] and numerical techniques for its solution[8] have been discussed elsewhere. The boundary condition imposed at the surface was[9]

$$L = K_L \cdot [n_S(x \to 0)]^2 \qquad (1)$$

where L is the number of D atoms released to the gas phase per unit area and time, $n_S(x \to 0)$ is the atomic density of D in solution just beneath the surface, and K_L is the temperature-dependent recombination coefficient.

In the above calculations the D diffusion coefficient was taken from the literature[1]. The concentration of strong He-associated traps was assumed to vary with depth as the calculated profile of He (Fig. 1), with 0.6 traps per He atom. The actual trap-to-He ratio is believed to lie within the range 0.5 - 1.0, since other values significantly degrade the quality of the fit to experiment. The binding enthalpy of the traps was adjusted to produce agreement with the first stage in the data given by open circles in Fig. 2, yielding 0.42 eV referenced to a solution site. This value has an estimated absolute uncertainty of $\pm$ 0.08 eV, due primarily to uncertainties in other system parameters such as number of traps and D diffusivity. Discussion of the coefficient K_L is deferred to the following section.

The data given by open triangles in Fig. 2 decrease over a relatively extended temperature range, in a fashion which suggests that defect traps in the near-surface implanted region were close to saturation. Consequently a similar experiment was performed with the D fluence reduced from 2 to 1 x 10^{16} at./cm^2, while the fluence of He implanted at 1.2 μm remained 6 x 10^{16} at./cm^2. The detrapping stage, in which D migrated from the near-surface defect traps to He traps at 1.2 μm, was indeed much sharper. It is given by open circles in Fig. 4, where the temperature scale is expanded from Fig. 2. The theoretical curve was fitted to the data with a defect trap strength of 0.22 eV. Two traps were assumed to be present for each implanted D; this ratio was necessarily $\gtrsim$1 to accommodate all of the D, and probably $\lesssim$2 because of the apparent saturation behavior for a fluence of 2 x 10^{16} D/cm^2. The estimated absolute uncertainty in the derived trap strength is $\pm$ 0.08 eV. A second theoretical curve in Fig. 4 gives the predicted behavior when the only traps within the material are those associated with He at 1.2 μm; clearly, defect traps must be present within the D-implanted region to explain the results. We suggest that the irradiation-defect traps observed here are vacancies.

Since mechanical deformation of type 304 stainless steel can introduce inclusions of martensite, we have considered the possibility that ion

implantation produces a similar transformation, and that this influences the observed trapping behavior. To determine whether such effects are significant, the experiment represented by open circles in Fig. 4 was repeated for type 310 stainless steel, where the austenitic (fcc) phase is much more stable, and the results are given by solid points in the same figure. The two detrapping stages are seen to be virtually identical. A similar result was obtained for detrapping from He bubbles. Moreover, transmission electron microscopy showed little if any transformation to martensite during He implantation of type 304 stainless steel.

In these proceedings Pontau et al., report an independent ion-beam study of He-associated D traps in stainless steel. Their results, although obtained by different methods, are consistent with our findings.

SURFACE RECOMBINATION

Surface release was characterized by first ion implanting 25 μm foils of type 304 stainless steel with 4×10^{16} at./cm^2 of 15 keV ^{4}He and 2×10^{16} at./cm^2 of 15 keV D. Specimen temperature was then increased rapidly into the range 425 - 575 K and subsequently held fixed. Nuclear reaction analysis with 700 keV ^{3}He was used periodically to determine the areal density of D remaining within the depth interval 0 - 0.4 μm, and from this both the D concentration in solution and the total quantity within the sample could be calculated using the results of the preceeding section. Before being mounted in the implantation/analysis chamber all foils were electropolished and exposed to air, so that oxide was present on the surface. In certain instances this oxide was removed from one face of the foil by in situ bombardment with 5×10^{16} at./cm^2 of 30 keV Fe (range ~10 nm) before the implantations of He and D. Some reoxidation of the sputtered surface is expected under the vacuum conditions of these experiments, $\lesssim 1.0 \times 10^{-5}$ Pa with the sample facing a liquid-nitrogen-temperature shield.

Figure 5 shows data from ion-sputtered stainless steel during isothermal annealing at 475 K. The plotted quantity is the areal density of D within the depth interval 0 - 0.4 μm, divided by the fluence implanted initially.

The continuing decrease with time resulted from two effects. First, D diffused from He-bubble traps into solution, producing near equilibrium between the occupancies of trap and solution sites in the thin foil within about 300 s. The second cause of the decrease was release to the gas phase at the surface, which continued over the duration of the experiment. Consequently the data in Fig. 5 depend directly upon the functional relationship between surface release and the D concentration in solution. The He traps simply provided a convenient and stable resevoir for D whose content could be readily measured.

The theoretical curve in Fig. 5 was obtained from the formalism discussed in the preceeding section, with the assumption that surface loss rate is given by Eq. 1. The data were fitted by adjusting only the recombination coefficient K_L, other model parameters being taken from the analysis of the temperature-ramp data in Figs. 2 and 4. This comparison between theory and experiment, in addition to yielding the value of K_L for the sputtered surface at 475 K, also confirms accurately that the kinetics of surface release are second order (Eq.1).

Figure 6 gives our results for the recombination coefficient with and without in situ sputtering of the surface oxide. (The latter values were used for the theoretical curves in Fig. 2.) Interestingly, the second-order kinetics of Eq. 1 were obeyed even in the presence of the strong oxide permeation barriers. The scatter in Fig. 6 is substantially greater than the relative uncertainty of the experimental determination, indicating differences among the surfaces of the samples. Indeed, in the case of measurements for the electropolished surface, points above the solid line are from three specimens electropolished in one batch, while points below the line are from two samples prepared at another time. Data for the two surface conditions in Fig. 6 approximately bracket previous results reviewed in Ref. 2, suggesting that the large discrepancies among earlier studies may in part derive from surface preparation. We nevertheless emphasize that our measurements extended to hours in a vacuum of 10^{-5} Pa, and consequently the values of K_L obtained after sputtering may not correspond to a bare metal surface; perhaps a higher vacuum would have yielded even larger K_L.

ACKNOWLEDGMENTS

The authors are indebted to C. R. Hills and W. R. Sorenson for performing the transmission electron microscopy and to J. C. Banks for invaluable technical assistance. This work was supported by the U. S. Department of Energy under Contract Number DE-AC0-4-76-DP00789. Sandia National Laboratories is a U. S. Department of Energy facility.

REFERENCES

[1] M. R. Louthan and R. G. Derrick, Corrosion Sci. 15 (1975) 565.

[2] K. L. Wilson, J. Nucl. Mater., in press

[3] S. M. Myers, F. Besenbacher, and J. Bøttiger, Appl. Phys. Lett. 39 (1981) 450, and to be published.

[4] F. Besenbacher, J. Bøttiger, and S. M. Myers, J. Appl. Phys., in press.

[5] J. P. Biersack and L. G. Haggmark, Nucl. Instrum. Methods 174 (1980) 257.

[6] D. K. Brice, Radiat. Eff. 11 (1971) 227.

[7] S. M. Myers, S. T. Picraux, and R. E. Stoltz, J. Appl. Phys. 50 (1979) 5710.

[8] S. M. Myers, D. E. Amos, and D. K. Brice, J. Appl. Phys. 47 (1976) 1812.

[9] I. Ali-Khan, K. J. Dietz, F. G. Waelbroeck, and P. Wienhold, J. Nucl. Mater. 76&77 (1978) 337.

FIGURE CAPTIONS

Fig. 1. Theoretically predicted implantation profiles for the experiment yielding open circles in Fig. 2.

Fig. 2. Deuterium retention versus temperature for stainless steel implanted with He and D. The implanted D fluence was 2×10^{16} at./cm^2, the ramp rate 2 K/min.

Fig. 3. Depth profile of D in the plateau between release stages. The implanted D fluence was 1×10^{16} at./cm^2.

Fig. 4. Deuterium retention versus temperature under conditions reflecting defect trapping. The implanted D fluence was 1×10^{16} at./cm^2.

Fig. 5. Surface release of D during isothermal annealing at 475 K. The vertical bar is ± the square root of proton counts for a representative data point, and is approximately the same for all points.

Fig. 6. Recombination coefficient with and without prior sputtering of surface oxide.

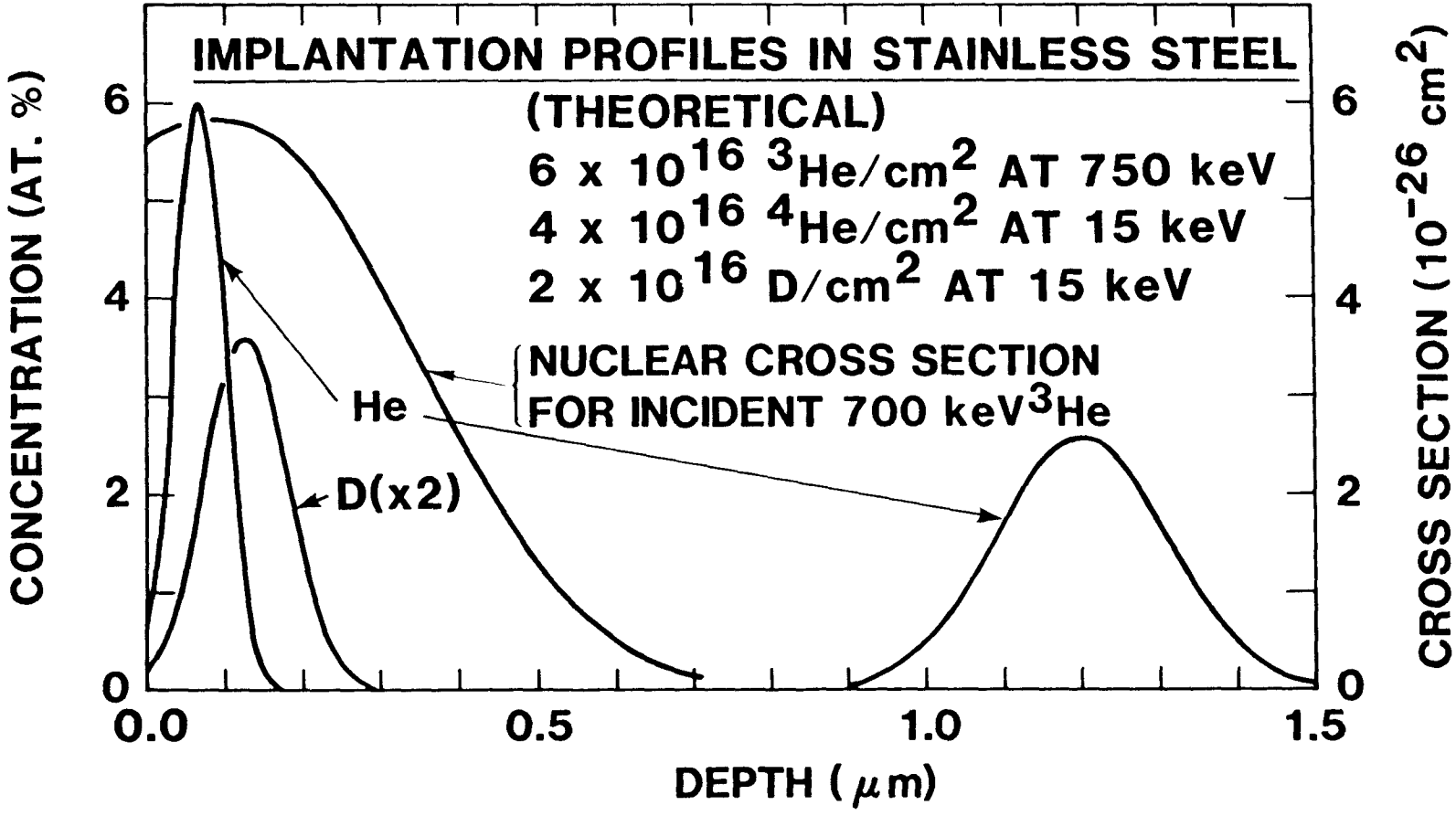
IMPLANTATION PROFILES IN STAINLESS STEEL
(THEORETICAL)
6 x 10^16 3He/cm^2 AT 750 keV
4 x 10^16 4He/cm^2 AT 15 keV
2 x 10^16 D/cm^2 AT 15 keV
NUCLEAR CROSS SECTION
FOR INCIDENT 700 keV 3He
He
D(x2)
CONCENTRATION (AT. %)
CROSS SECTION (10^-26 cm^2)
DEPTH (μm)
0
2
4
6
0.0
0.5
1.0
1.5

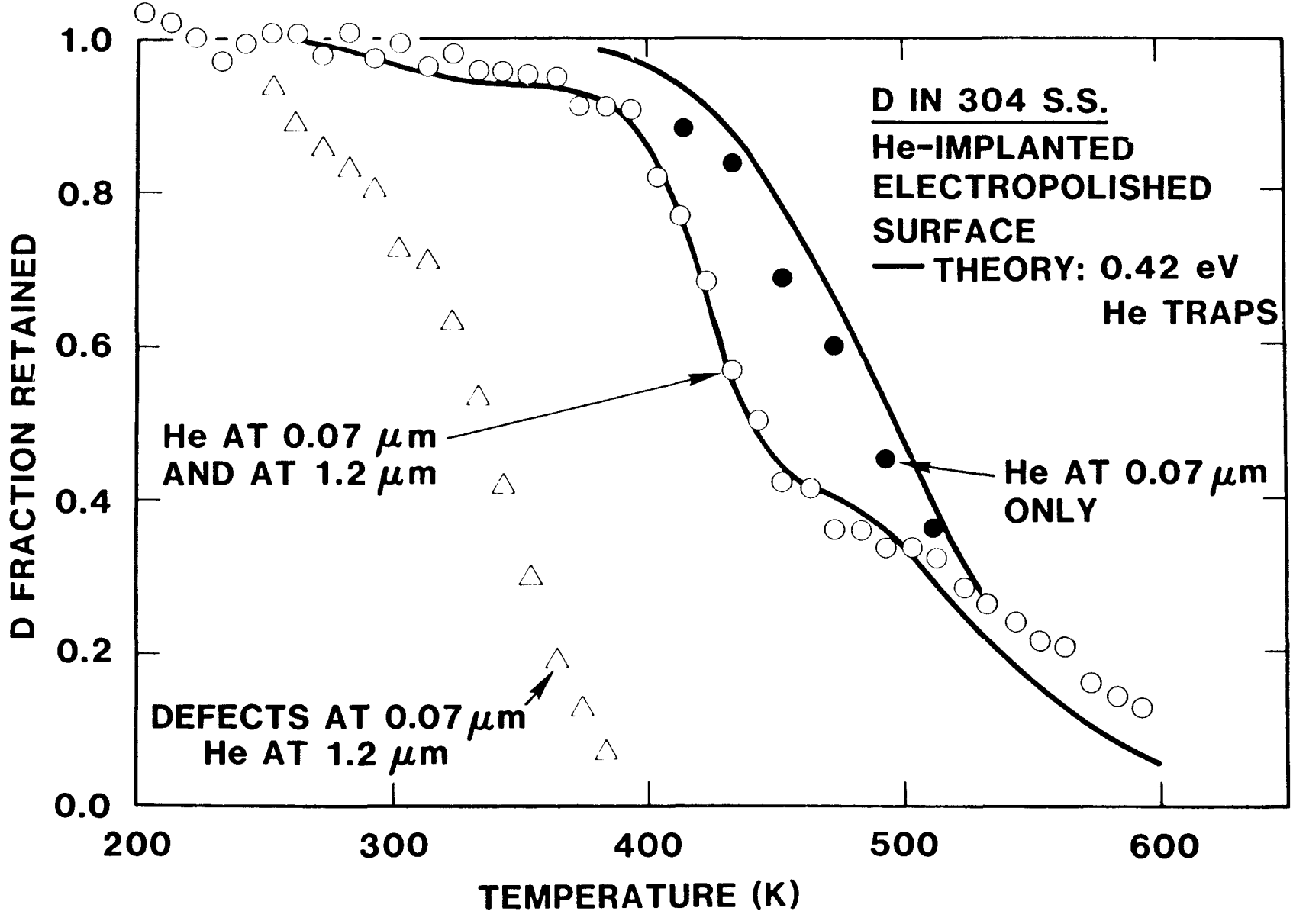
D IN 304 S.S.
He-IMPLANTED
ELECTROPOLISHED
SURFACE
THEORY: 0.42 eV
He TRAPS
He AT 0.07 μm
AND AT 1.2 μm
He AT 0.07 μm
ONLY
DEFECTS AT 0.07 μm
He AT 1.2 μm
D FRACTION RETAINED
TEMPERATURE (K)
1.0
0.8
0.6
0.4
0.2
0.0
200
300
400
500
600

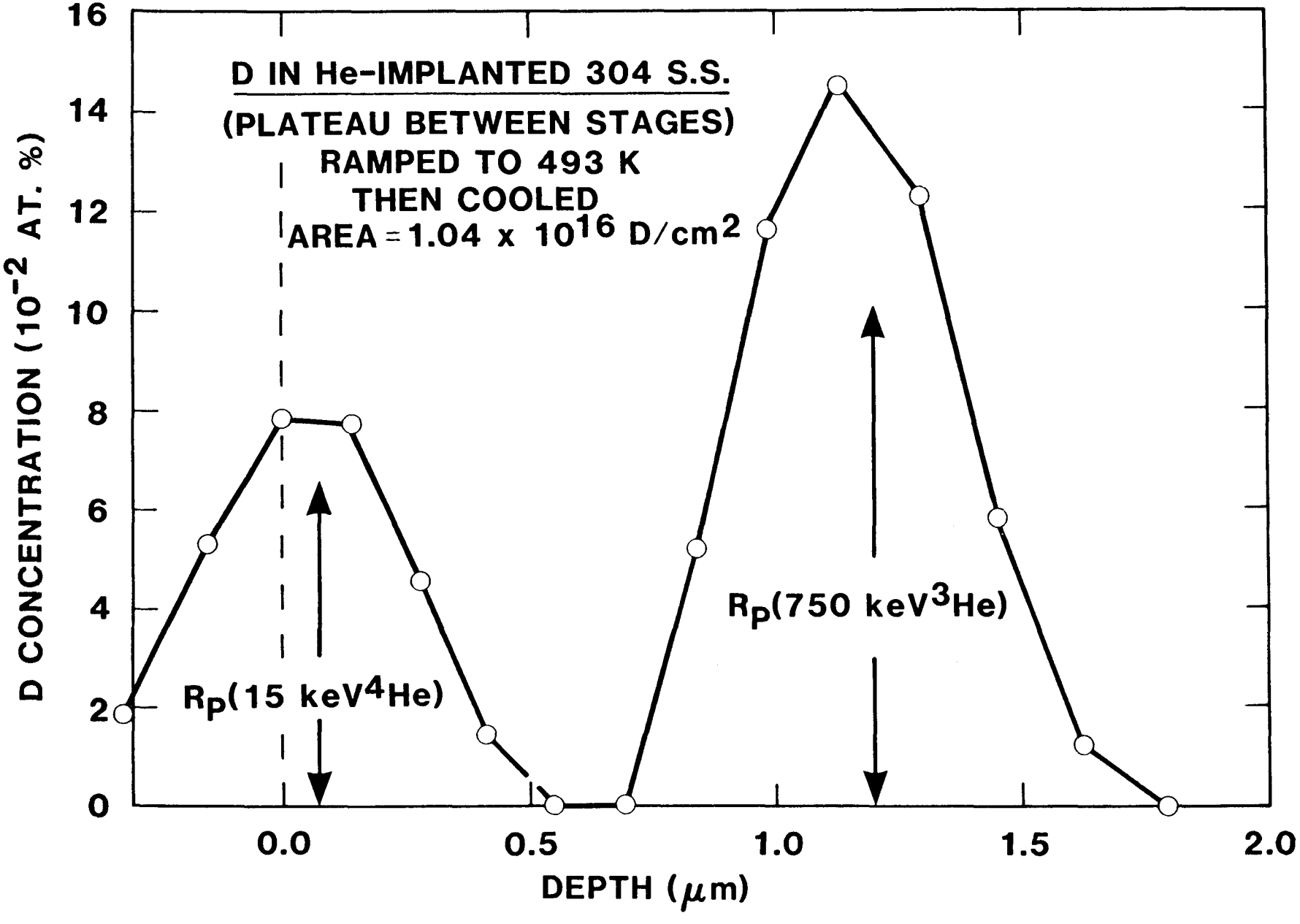
D IN He-IMPLANTED 304 S.S.
(PLATEAU BETWEEN STAGES)
RAMPED TO 493 K
THEN COOLED
AREA = 1.04 x 10^16 D/cm^2
D CONCENTRATION (10^-2 AT. %)
DEPTH (μm)
R_P(15 keV 4He)
R_P(750 keV 3He)
0
2
4
6
8
10
12
14
16
0.0
0.5
1.0
1.5
2.0

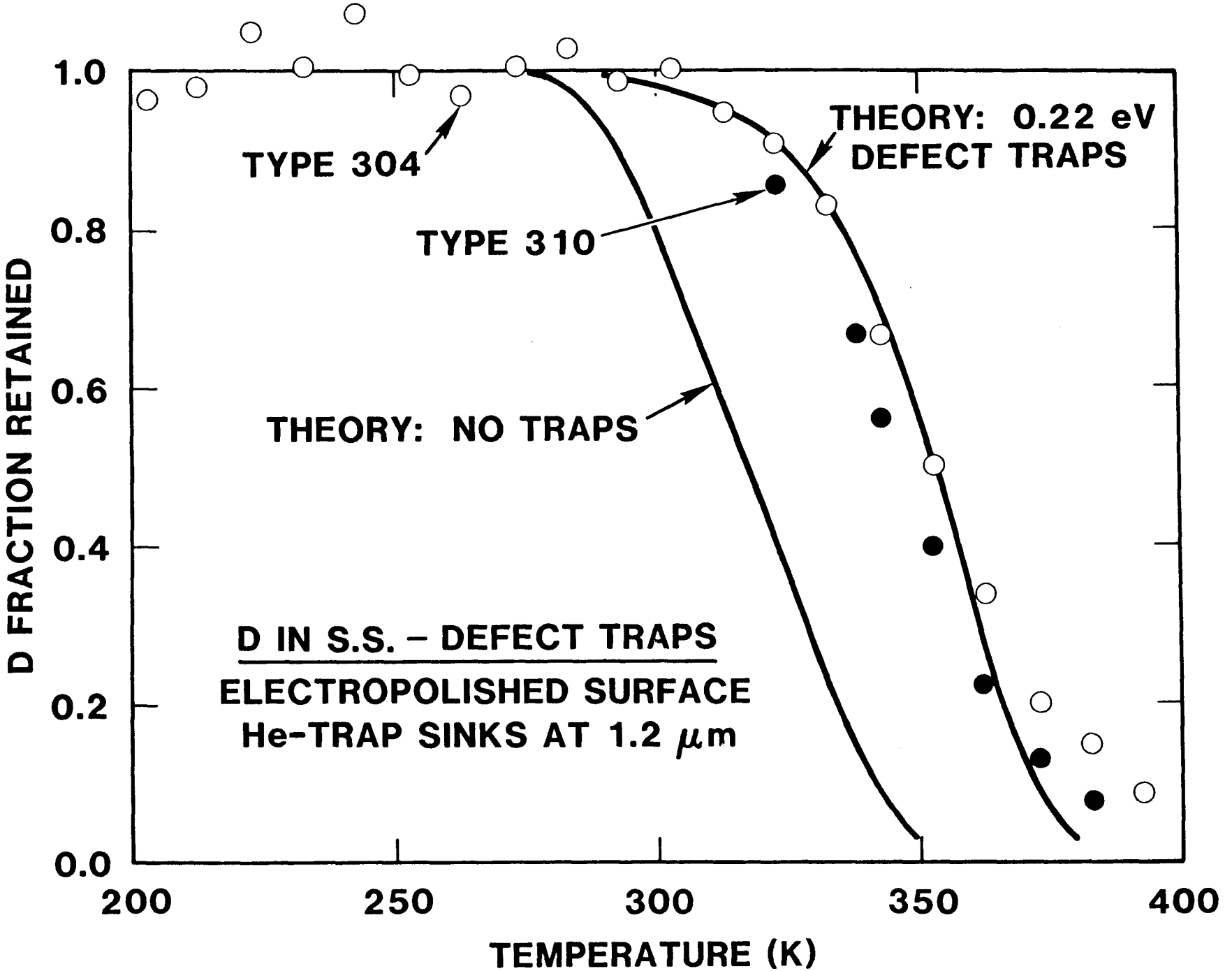
1.0
0.8
0.6
0.4
0.2
0.0
D FRACTION RETAINED
200
250
300
350
400
TEMPERATURE (K)
TYPE 304
TYPE 310
THEORY: 0.22 eV
DEFECT TRAPS
THEORY: NO TRAPS
D IN S.S. – DEFECT TRAPS
ELECTROPOLISHED SURFACE
He-TRAP SINKS AT 1.2 μm

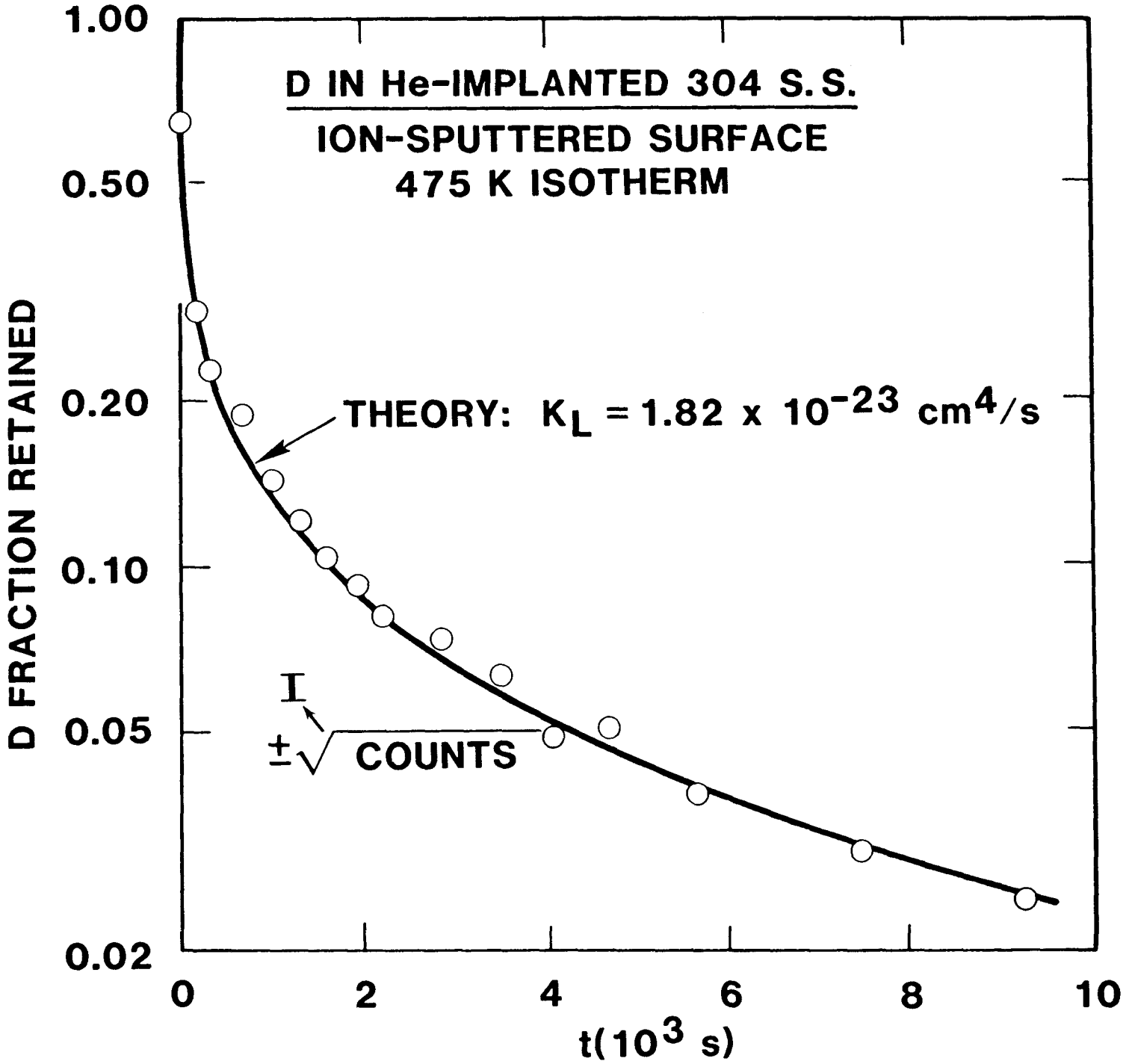
D IN He-IMPLANTED 304 S.S.
ION-SPUTTERED SURFACE
475 K ISOTHERM
THEORY: $K_L = 1.82 \times 10^{-23}$ cm^4/s
$\pm\sqrt{I}$ COUNTS
D FRACTION RETAINED
1.00
0.50
0.20
0.10
0.05
0.02
0
2
4
6
8
10
t(10^3 s)

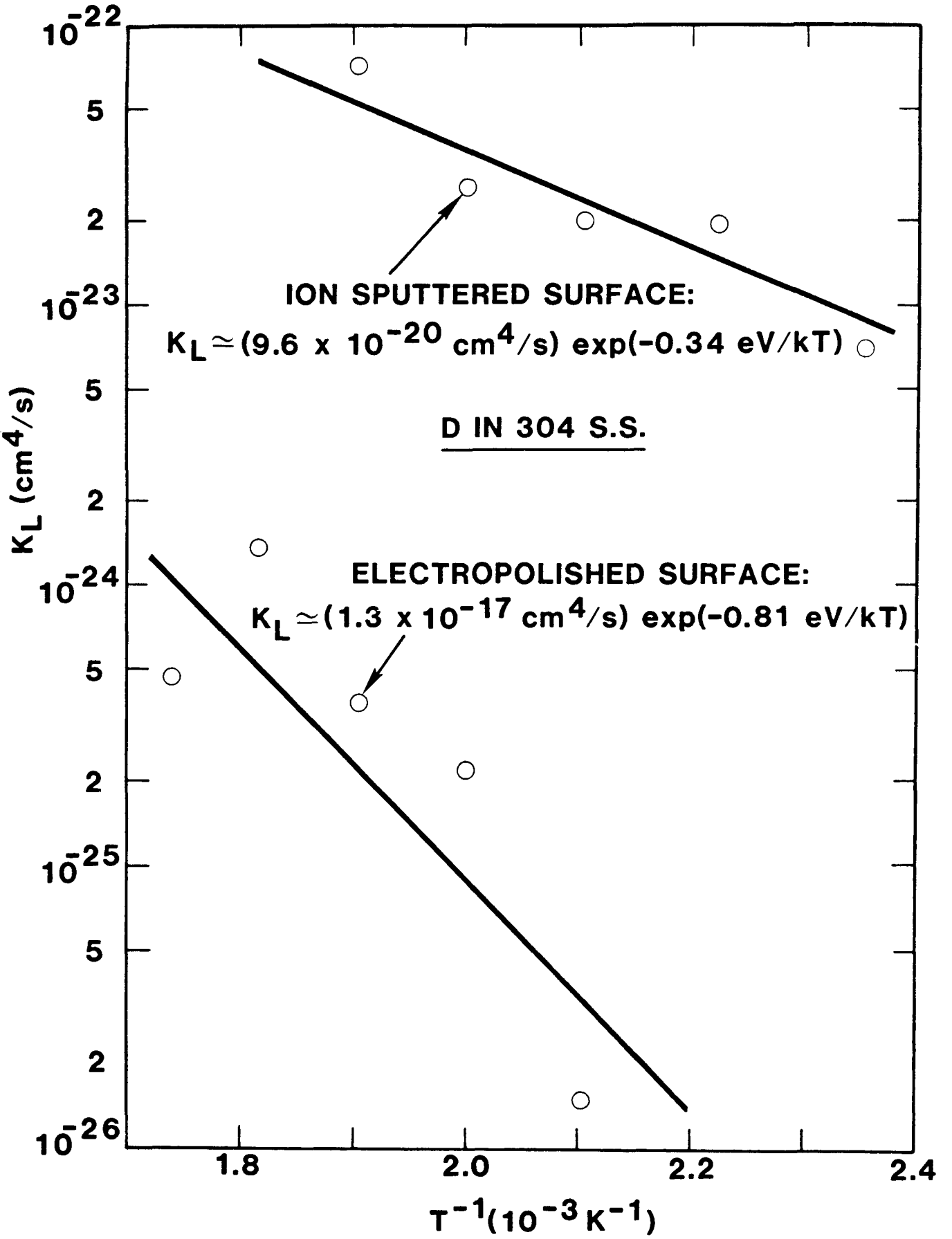
ION SPUTTERED SURFACE:
$K_L \simeq (9.6 \times 10^{-20}\ cm^4/s)\ exp(-0.34\ eV/kT)$
D IN 304 S.S.
ELECTROPOLISHED SURFACE:
$K_L \simeq (1.3 \times 10^{-17}\ cm^4/s)\ exp(-0.81\ eV/kT)$
$K_L\ (cm^4/s)$
10^{-22}
5
2
10^{-23}
5
2
10^{-24}
5
2
10^{-25}
5
2
10^{-26}
1.8
2.0
2.2
2.4
$T^{-1}(10^{-3}\ K^{-1})$